Transition-State Theory and Secondary Forces in Antigen−Antibody Complexes

Mark E. Mummert and Edward W. Voss, Jr.*

Department of Microbiology, University of Illinois, 131 Burrill Hall, 407 South Goodwin Avenue, Urbana, Illinois 61801-3704

Received February 27, 1996; Revised Manuscript Received April 25, 1996[⊗]

ABSTRACT: Secondary forces, defined as those interactions between the antigen (epitope including the surrounding environment) and areas immediately adjacent to the antibody active site, were investigated using monofluorescein-derivatized synthetic peptides of varying electrostatic properties. Secondary forces were quantitated by measuring the unimolecular rate constants at two different temperatures using the high-affinity anti-fluorescein monoclonal antibody 4-4-20 complexed with fluorescein-derivatized synthetic peptides. Unimolecular rate constants were correlated with transition-state theory to explain secondary effects. An acidic peptide produced a large temperature-dependent effect upon binding including a significant enthalpic factor (+33.28 kcal/mol) relative to the binding of fluorescein ligand (+23.96 kcal/mol). Binding of a basic peptide produced both a relatively smaller temperature effect and enthalpy factor than fluorescein ligand. The antibody−ligand binding results were interpreted invoking the concepts of thermally averaged metatypic (liganded) states of the antibody as well as potential biochemical interactions between the antigen and accessible surface regions of the antibody's complementarity determining regions.

It was previously demonstrated that antigen binding efficiency and variable domain conformational states of the high-affinity anti-fluorescyl monoclonal antibody 4-4-20 were modulated by interactions external to the antibody active site per se (Mummert & Voss, 1995, 1996). Antigen for these purposes was defined as an epitope plus the surrounding environment as in a macromolecule. Interactions within the antibody active site, which dictate ligand specificity, represent primary interactions while interactions immediately outside the antibody active site, which modulate binding, have been termed secondary forces. Although secondary effects do not directly govern specificity, they exert significant effects on the free energy of binding as well as on the spectral and kinetic properties of the antibody/ligand interaction (Absolom & van Oss, 1986; Mummert & Voss, 1995, 1996). Investigations into the interaction of mAb 4-4-20 with various synthetic monofluoresceinated peptides revealed additive changes in the free energy of binding as great as 2 kcal/mol relative to the binding of fluorescein ligand (Mummert & Voss, 1996). Secondary forces therefore constitute important contributions when considering the intricacies of antibody active site/ligand interactions. Indeed, it has been proposed that the stability of antigen−antibody complexes can be more accurately evaluated as a summation (either positive or negative) of primary and secondary interactive components (Mummert & Voss, 1996).

Mummert and Voss (1995, 1996) investigated effects of secondary forces utilizing mAb 4-4-20 with monofluoresceinated proteins and synthetic peptides. mAb 4-4-20 was considered an ideal model to evaluate secondary forces since fluorescein had been determined to be an active site-filling moiety for mAb 4-4-20 based on X-ray crystallographic analyses (Herron *et al.*, 1989, 1994; Whitlow *et al.*, 1995). Calculations based on the resolved three-dimensional structure (<2.0 Å) indicated that only ∼7% of the fluorescein ligand surface area was solvent-accessible when bound within the relatively deep active site pocket of mAb 4-4-20 (Whitlow *et al*., 1995). This relative inaccessibility was consistent with iodide fluorescence (dynamic) quenching studies with fluorescein bound to 4-4-20 (Coelho-Sampaio & Voss, 1993). Changes in the binding free energy of fluoresceinated peptide derivatives relative to fluorescein were therefore assumed to be due to interactions (either attractive or repulsive) occurring outside the active site pocket. Moreover, upon binding with mAb 4-4-20, the fluorescein ligand and various monofluoresceinated peptides displayed a bathochromic shift in absorbancy while the fluorescein and mAb 4-4-20 intrinsic tryptophan fluorescence was quenched (Mummert & Voss, 1996) to different degrees. Therefore, variable domain perturbations induced by interactions supplemental to the primary interaction could be quantitated for the monofluoresceinated derivatives and compared to fluorescein ligand devoid of secondary interactions. It was further reasoned that studies of secondary forces may provide a mechanism to experimentally induce and resolve various conformational states.

Models have been proposed to account for the observed experimental results (Mummert & Voss, 1995, 1996; Carrero & Voss, 1996). These models were based on the premise that an unliganded active site (idiotype) existed in solution as a dynamic series of conformational substates separated by energetic barriers that were not prohibitively large (Figure 1). Upon antibody interaction with a homologous ligand, a transitory encounter complex formed. Kinetic analyses of the antibody−ligand interaction revealed a two-step association reaction in both heterogeneous and homogeneous antibody populations (Voss, 1993). Subsequent to formation of the encounter complex, it was postulated that the complementarity determining regions (CDRs)[1] within the antibody

* To whom correspondence should be addressed. Phone: (217)333-0299 or (217)333-1738. Fax: (217) 244-6697. E-mail: e-voss@uiuc.edu.

[⊗] Abstract published in *Advance ACS Abstracts,* June 1, 1996.

[1] Abbreviations: FDS, fluorescein disodium salt; Fl-NH_2, fluorescein amine isomer I; RP-HPLC, reverse-phase high-pressure liquid chromatography; CDR, complementarity determining region.

S0006-2960(96)00479-5 CCC: $12.00

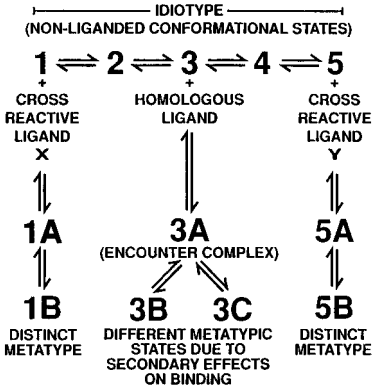

FIGURE 1: Dynamic conformational state model of immunoglobulin variable domains. The unliganded idiotype state is indicated arbitrarily as states 1 through 5 which exist in a dynamic equilibrium. Homologous ligand interacts preferentially with state 3 which is a dominant energetically favorable state in a Gaussian distribution (Voss *et al.*, 1988). States 1 and 5 are depicted as relatively extreme conformational states which react relatively weakly with the homologous ligand but bind various cross-reactive ligands efficiently. The various stable metatypic liganded states 1B and 5B represent distinct conformations relative to states 3B and 3C. The latter differ based on secondary effects on conformation.

variable domains undergo conformational changes resulting in the final thermally averaged liganded conformational state (metatypic state). The relatively stable metatypic state determined the properties of the variable domains (i.e., spectral, kinetic, and energetic) upon binding a given ligand. Thus, in previous studies the metatypic conformational state was assumed to have been modulated by secondary forces as inferred from spectral and kinetic analyses as well as by the use of specific polyclonal antimetatype (i.e., anticonformational state antibodies) antibody reagents (Mummert & Voss, 1996). Dynamic models of proteins such as antibodies are considered more biologically appropriate than static models (Ansari *et al.*, 1992; Hagen *et al.*, 1995).

To gain deeper insight into secondary forces and to enhance model development for the mechanism of secondary forces, the stability of mAb 4-4-20 complexed with fluorescein or a synthetic monofluoresceinated peptide was quantitated by measuring the unimolecular rate constant at two different temperatures. Overall, the reaction for the experimental system employed can be considered a displacement reaction as in eq 1

$$AB + C \rightarrow AC + B \quad (1)$$

where A is antibody, B is fluorescein or a monofluoresceinated peptide, AB is the antibody/fluorescein or antibody/monofluoresceinated peptide complex, C is a nonfluorescent analog (fluoresceinamine), and AC is the antibody/fluoresceinamine complex. Utilizing a large excess of fluoresceinamine relative to bound fluorescein or one of the monofluoresceinated peptides, the decay of the antibody/fluorescein complex was essentially unidirectional (Herron, 1984). The rate of complex decomposition was used to calculate thermodynamic transition-state parameters (Moore & Pearson, 1981). The general equation relating reactants, the transition state, and product is

$$A + B \leftrightarrow AB^{\ddagger} \leftrightarrow AB \quad (2)$$

where A is antibody, B is ligand, $AB^{\ddagger}$ is the transition state, and AB is the antibody/ligand complex including the final conformational change. $AB^{\ddagger}$ represents the energy maximum of the reaction along the reaction coordinate. The height of

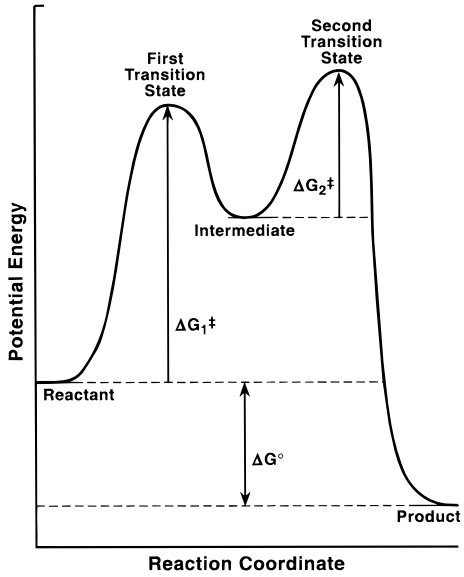

FIGURE 2: Two-dimensional reaction coordinate depicting the interaction of mAb 4-4-20 with homologous ligand. The *x*-axis is the arbitrarily assigned reaction progression while the *y*-axis is the chemical potential. The height of the chemical potential barriers dictates the rate of the reaction. The encounter complex was included in the model to account for the experimentally observed results of the unimolecular rate constant (Herron, 1984).

the energy maximum (i.e., the energy barrier) determines the rate of the reaction. Previous models infer two transition-state free energy maxima due to inclusion of an encounter complex (Mummert & Voss, 1995, 1996). The two-dimensional reaction coordinate predicted by these models is illustrated in Figure 2.

These studies were designed to use transition-state theory as a means to derive the mechanism of secondary forces. Results of the studies presented have been interpreted within the theoretical framework of thermally averaged metatypic states as well as potential biochemical interactions between accessible surface regions of the CDRs and amino acids comprising the monofluoresceinated peptides.

MATERIALS AND METHODS

Peptide Synthesis. Synthesis of amino-terminal acetylated monofluoresceinated peptides has been described in detail elsewhere (Mummert & Voss, 1996). Briefly, peptide construction followed the general design: Ac-NH-X-X-X-X-X-X-LYS-X-X-X-X-X-X-COO- where Ac-NH represents the acetylated α-amino group, X represents aspartic acid or arginine amino acids, and LYS is the central lysyl residue. Fluorescein 5-isothiocyanate (or isomer I) was covalently coupled to the ϵ-amine of the lysine residue. Purification and verification of synthesis of the monofluoresceinated peptides have been previously described (Mummert & Voss, 1996).

Monoclonal Antibody 4-4-20. The properties of mAb 4-4-20 have been summarized in Mummert and Voss (1996). Briefly mAb 4-4-20 (IgG2a, K) has an affinity for fluorescein of 2×10^{10} M^{-1} and quenches bound fluorescein ligand 96%. The thermodynamic properties of mAb 4-4-20 have been described by Herron *et al.* (1986). The crystal structure of mAb 4-4-20 at <2.0 Å was described by Herron *et al.* (1994) and Whitlow *et al.* (1995).

mAb 4-4-20 was produced from ascitic fluid in pristane-treated Balb/c mice (Kranz & Voss, 1981). After centrifugation of ascites fluid to sediment cells, immunoglobulin

enrichment was accomplished by dextran sulfate precipitation of lipoproteins followed by ammonium sulfate (50% saturated) precipitation. Active and specific antibody was affinity-purified using a fluorescein−Sepharose 4B adsorbent (Weidner *et al.*, 1993). Antibody elution was accomplished with glycine−NaCl buffer, pH 2.3 (50 mM glycine, 150 mM NaCl). The affinity-purified fraction was subjected to exhaustive dialysis against 100 mM phosphate, pH 8.0, and the purity was verified utilizing SDS−PAGE and RP-HPLC. Previous studies using circular dichroism and ligand binding analysis have shown that when mAb 4-4-20 is eluted at pH 2.3 there are no detectable changes in the antibody molecule (Tetin *et al.*, 1992).

Determination of Unimolecular Rate Constants. Ligand dissociation rates were determined at 275 and 291 K as described by Herron (1984). Briefly, a 10-fold molar excess of antibody active sites was added to a solution of fluorescein or a monofluoresceinated peptide in a cuvette (100 μL total volume). Upon equilibration for 10 min at 275 or 291 K, the volume was adjusted to 1 mL by rapid addition of a 5- or 10-fold molar excess (relative to moles of active site) of Fl-NH_2 (fluorescein amine analog with a low quantum yield fluorescence) in 100 mM phosphate, pH 8.0. Increased fluorescence with time was monitored continuously with an Aminco-Bowman spectrofluorometer and a direct data feed into an IBM PC. Samples were excited at 480 nm, and fluorescence emission was monitored through a 510 nm cutoff filter at 530 nm. Temperature was maintained using a Grant LTD 6 controlled bath and circulator. Ligand dissociation rates were determined by the computer program OFFRATES, version 1.2 (Interactive Software, Urbana, IL), from the slope of plots utilizing the equation:

$$\ln [(FU_m - FU_t)/(FU_m - FU_o)](t)^{-1} = -k_2 \qquad (3)$$

where FU_m is the maximum fluorescence observed, FU_o is the initial fluorescence intensity observed, FU_t is the fluorescence observed at time t, and k_2 is the unimolecular rate constant.

Calculation of Transition-State Thermodynamic Parameters. Activation energy was determined from the equation:

$$E_a = RT_2T_1/T_2 - T_1 (\ln k_2/k_1) \qquad (4)$$

where E_a is the activation energy, R is the gas constant, T_1 and T_2 are absolute temperatures, and k_1 and k_2 are the experimentally determined unimolecular rate constants at T_1 and T_2, respectively.

Enthalpic transition-state parameters were calculated from the equation:

$$\Delta H^{\ddagger} = E_a - RT \qquad (5)$$

where the symbol ‡ designates the transition state with all components in their standard state. $\Delta H^{\ddagger}$ is the transition-state enthalpy, E_a is the activation energy, R is the gas constant, and T is the absolute temperature.

Entropic transition-state parameters were determined from the equation:

$$\Delta S^{\ddagger} = R (\ln Ah/k_BT - 1) \qquad (6)$$

where $\Delta S^{\ddagger}$ is the transition-state entropy, h is the Planck's constant, k_B is the Boltzmann constant, T is absolute temperature, and A is the Arrhenius preexponential factor determined from the equation:

$$\ln k = -E_a/RT + \ln A \qquad (7)$$

where k is the experimentally determined unimolecular rate constant, E_a the activation energy, R the gas constant, and T the absolute temperature.

Free energy of activation was determined from the equation:

$$\Delta G^{\ddagger} = \Delta H^{\ddagger} - T\Delta S^{\ddagger} \qquad (8)$$

where $\Delta G^{\ddagger}$ is the transition-state free energy, $\Delta H^{\ddagger}$ the transition-state enthalpy, $\Delta S^{\ddagger}$ the transition-state entropy, and T the absolute temperature.

The equilibrium for formation of the transition state was determined from the equation:

$$K^{\ddagger} = \exp(-\Delta G^{\ddagger}/RT) \qquad (9)$$

where $\Delta G^{\ddagger}$ is the activation free energy, R the gas constant, and T the absolute temperature.

The value for the transmission coefficient was calculated from the relation:

$$k = \kappa(RT/N_Ah)K^{\ddagger} \qquad (10)$$

where k is the reaction rate, T the absolute temperature, h the Planck constant, R the gas constant, $K^{\ddagger}$ the transition-state equilibrium constant, N_A the Avogadro constant, and κ the transmission coefficient. Transition-state theory assumes that κ is unity which is a fundamental theoretical assumption (Winger, 1938). Insight into the reaction mechanism as a result of the failure of this fundamental assumption of transition-state theory will be presented under Discussion.

RESULTS

Affinity of mAb 4-4-20 with Various Ligands. In previous studies (Mummert & Voss, 1996) the association (affinity) constants for the interaction of mAb 4-4-20 with fluorescein and the monofluoresceinated peptides were measured at 275 K. The affinities of 4-4-20 for FDS, D12KFl, R12KFl, and R6D6KFl were 3.14×10^{10} M^{-1}, 1.49×10^9 M^{-1}, 7.55×10^8 M^{-1}, and 7.49×10^8 M^{-1}, respectively, as shown in Table 1.

Unimolecular Rate Constants. Unimolecular rate constants for decay of the mAb 4-4-20/fluorescein complex and for the various mAb 4-4-20/monofluoresceinated peptide complexes were determined at 275 and 291 K. The 16 K temperature differential resulted in significant changes in the various decay rates of the various complexes. In all cases, the unimolecular rate constant increased with higher temperature. The largest change with temperature was noted with mAb 4-4-20 and D12KFl (30.3-fold). While the

Table 1: Comparative Unimolecular Rate Constants at 275 and 291 K for the Interaction of FDS and Monofluoresceinated Peptides with mAb 4-4-20

ligand	K_a (M^{-1})[c]	k_{-1}[a]	k_{-1}[b]	k_{-1}^a/k_{-1}^b
FDS	3.14×10^{10}	$1.63 (\pm 0.02) \times 10^{-4}$	$1.92 (\pm 0.09) \times 10^{-3}$	12.0
D12KFl	1.49×10^9	$3.52 (\pm 0.62) \times 10^{-3}$	$1.06 (\pm 0.19) \times 10^{-1}$	30.3
R6D6KFl	7.55×10^8	$6.96 (\pm 1.02) \times 10^{-3}$	$1.15 (\pm 0.42) \times 10^{-1}$	16.7
R12KFl	7.49×10^8	$6.79 (\pm 0.25) \times 10^{-3}$	$6.08 (\pm 0.81) \times 10^{-2}$	8.9

[a] Unimolecular rate constant at 275 K. [b] Unimolecular rate constant at 291 K. [c] K_a = affinity values taken from Mummert and Voss (1996).

Table 2: Comparative Thermodynamic Transition-State Parameters and Transition-State Equilibria for the Interaction of mAb 4-4-20 with FDS and Monofluoresceinated Peptides at 275 K[a]

ligand	$\Delta H^{\ddagger}$	$\Delta S^{\ddagger}$	$\Delta G^{\ddagger}$	$K^{\ddagger}$
FDS	$+23.96 \pm 0.06$	$+0.01 \pm 0.00$	$+20.82 \pm 0.07$	2.84×10^{-17}
D12KFl	$+33.28 \pm 1.95$	$+0.05 \pm 0.00$	$+19.15 \pm 1.95$	6.03×10^{-16}
R6D6KFl	$+27.32 \pm 3.36$	$+0.03 \pm 0.00$	$+18.77 \pm 3.36$	1.21×10^{-15}
R12KFl	NA	NA	NA	NA

[a] $\Delta H^{\ddagger}$ = transition-state enthalpy (kcal/mol). $\Delta S^{\ddagger}$ = transition-state entropy (kcal^{-1} mol^{-1} deg^{-1}). $\Delta G^{\ddagger}$ = transition-state free energy (kcal/mol). $K^{\ddagger}$ = transition-state equilibrium (the equilibrium constant is dimensionless). NA = not applicable; does not conform to the theoretical assumptions of transition-state theory.

Table 3: Comparative Differences in Thermodynamic Transition-State Parameters of Monofluoresceinated Peptides with Respect to FDS at 275 K[a]

ligand	$\Delta\Delta H^{\ddagger}$	$\Delta\Delta S^{\ddagger}$	$\Delta\Delta G^{\ddagger}$
D12KFl	$+9.32 \pm 1.95$	$+0.04 \pm 0.00$	-1.67 ± 1.95
R6D6KFl	$+3.36 \pm 3.36$	$+0.02 \pm 0.00$	-2.05 ± 3.36
R12KFl	NA	NA	NA

[α] $\Delta\Delta H^{\ddagger}$ = change in the transition-state enthalpy with respect to FDS (kcal/mol). $\Delta\Delta S^{\ddagger}$ = change in the transition-state entropy with respect to FDS (kcal^{-1} mol^{-1} deg^{-1}). $\Delta\Delta G^{\ddagger}$ = change in the transition-state free energy with respect to FDS (kcal/mol). NA = not applicable.

antibody interaction with R12KFl showed a smaller change with temperature than with the FDS ligand (8.9-fold vs 12.0-fold), importantly the R6D6KFl ligand gave a 16.7-fold change which is the approximate average of the changes noted with D12KFl (polyanion) and R12KFl (polycation).

At the two temperatures utilized for these experiments (275 and 291 K), it was assumed that complexes moved over energetic barriers with standard Arrhenius motion. Deviations from Arrehenius motion (e.g., tunneling) usually result as a consequence of low temperature (Frauenfelder *et al.*, 1991; Wolynes, 1987; Frauenfelder, 1979). Equations utilized for data analyses are described in more detail in Moore and Pearson (1981).

Relationship between Enthalpy and Entropy. When the temperature differences were analyzed in terms of thermodynamic parameters, significant changes in $\Delta H^{\ddagger}$ for the various fluorescent probes complexed with mAb 4-4-20 were observed (Tables 2 and 3) with minimal changes in $\Delta S^{\ddagger}$. D12KFl and potentially R6D6KFl indicated $\Delta H^{\ddagger}$ values that appeared enhanced relative to FDS. Similarly, $\Delta S^{\ddagger}$ values for D12KFl and R6D6KFl indicated enhancement relative to FDS (Tables 2 and 3). The value for $\Delta G^{\ddagger}$, however, was greatest in the decay rate of the mAb 4-4-20/FDS complex devoid of secondary forces.

κ Values. Values for κ (transmission coefficient) were 1.00, 1.02, 1.00, and 0.58 for FDS, D12KFl, R6D6KFl, and R12KFl, respectively. The κ value was indicative of the approximation between transition-state theory and the calculated transition-state thermodynamic parameters. Transition-state theory assumes unity for κ. Deviations of κ from unity indicated poor approximation of the various transition-state thermodynamic parameters. Thus, all immune complex decay rates were adequately described by transition-state theory except for peptide R12KFl. As noted previously, R12KFl produced a smaller effect with temperature than FDS and may be correlated with the κ value of less than unity. The potential ramifications of these results are addressed under Discussion.

DISCUSSION

Because of the physiological and biomedical importance of antibody−ligand interactions (Miklasz *et al.*, 1995), it is important to comprehensively evaluate all parameters that influence antibody recognition and binding events. Secondary forces have been shown to represent significant perturbations in determining the stability of antibody−antigen complexes, but their mechanism of action remains undefined (Mummert & Voss, 1995, 1996). Since transition-state theory allows for conceptual development of reaction mechanisms, these studies attempted to evaluate secondary forces within the framework of transition-state theory (Eyring, 1935; Wynne-Jones & Eyring, 1935).

Accuracy of transition-state values increases with increasing temperature intervals (Hasha *et al.*, 1982). Due to technical limitations in the instrumentation utilized for these experiments, only two temperatures were evaluated. These data must therefore be considered average values for $\Delta G^{\ddagger}$, $\Delta H^{\ddagger}$, and $\Delta S^{\ddagger}$at 275 K. However, the values obtained are meaningful relative to one another and are at least qualitatively relevant.

Consistent with transition-state theory, differences in the unimolecular rate constants (Table 1) and the resulting thermodynamic parameters (Table 2) were measured. It was evident that relative to the interaction of mAb 4-4-20 with fluorescein and the various fluorescein peptides that the conjugated peptide ligands exerted significant secondary effects.

As shown in Table 1, the effect of temperature on the unimolecular rate constant varied with the electrostatic nature of the ligand. In the case of fluorescein the temperature effect on the rate constant between 275 and 291 K was 12-fold. The three fluoresceinated peptides D12KFl, R6D6KFl and R12KFl varied with temperature by 30.2-fold, 16.5-fold, and 8.9-fold, respectively. Binding results with the hybrid ligand R6D6KFl (16.5-fold) represented the approximate average between the temperature differences obtained with D12KFl and R12KFl. These results can be viewed as a titration of effects of either the anionic or the cationic groups. Relative effects on the rate constants can also be correlated with the various antibody affinities as noted in Table 1. In this context, the affinity of mAb 4-4-20 for D12KFl was reduced approximately 20-fold (3.14×10^{10} M^{-1} to 1.49×10^{9} M^{-1}). Whereas the affinity of mAb 4-4-20 for R6D6KFl (7.55×10^{8} M^{-1}) and R12KFl (7.49×10^{8} M^{-1}) was reduced 42-fold relative to fluorescein ligand or only 2-fold relative to D12KFl. Thus, temperature-dependent differences in unimolecular rate constants did not correlate directly with differences in antibody affinities.

Such differences and effects can also be analyzed on the basis of thermodynamic parameters, and for this reason, relative values for enthalpy and entropy were measured (Table 2). In terms of the $\Delta H^{\ddagger}$ and $\Delta S^{\ddagger}$ thermodynamic parameters, the most significant effects were noted in the $\Delta H^{\ddagger}$ values. Effects of peptide R12KFl on binding were disregarded because the κ value was 0.58 (i.e., less than unity). Thus, for FDS, D12KFl, and R6D6KFl, the $\Delta H^{\ddagger}$ values were +23.96, +33.28, and +27.32 kcal/mol, respectively.

Unequal transition-state values of $\Delta H^{\ddagger}$ and $\Delta S^{\ddagger}$ of the various complexes evaluated were indicative of fundamental differences in bonding interactions for the activated intermediates. We proposed that differences in the bonding

Table 4: Summary of Properties Defining the Interaction of mAb 4-4-20 with Fluorescein- and Monofluorescein-Labeled Synthetic Polypeptides

ligand	K_a (M^{-1})[a]	λ_{max}[b] (nm)	Q_{max} ligand[c] (%)	Q_{max} tryptophan[d] (%)	Met + anti-Met (M^{-1})
FDS	3×10^{10}	505	88.0	65.7	2×10^{11}
D12KFl	1.5×10^{9}	505	51.5	75.5	2×10^{11}
D6R6KFl	7.5×10^{8}	502	43.0	73.0	2×10^{11}
R12KFl	7.5×10^{8}	500	76.0	70.0	2×10^{11}

[a] Affinities as reported in Mummert and Voss (1996). [b] Wavelength of maximum absorption of bound fluorescein. [c] Maximum fluorescence quenching of bound fluorescein expressed as percent quenching. [d] Maximum fluorescence quenching of tryptophan residues in mAb4-4-20 upon saturation with a given ligand.

networks of the various probes with the CDRs of mAb 4-4-20 provided plausible models to account for these results. It is important to stress that model development was based on the following observations: (1) FDS has been determined to be a site-filling moiety for mAb 4-4-20 (Whitlow *et al.*, 1995); (2) theoretical isoelectric point calculations indicated that the six CDRs of mAb 4-4-20 have relatively extreme cationic and anionic properties (Voss, 1993; Gulliver *et al.*, 1995); and (3) a significant percentage of the amino acids that comprise the mAb 4-4-20 CDRs are solvent-accessible when fluorescein is in the active-site (Whitlow *et al.*, 1995). Based on these results, we considered interactions (either repulsive or attractive) between regions of the CDRs outside of the active-site per se and amino acids constituting the synthetic peptides to be a reasonable assumption.

The results were analyzed in terms of specific models. The first model proposed that the enhanced values of $\Delta H^{\ddagger}$ and $\Delta S^{\ddagger}$ of mAb 4-4-20/D12KFl and mAb 4-4-20/R6D6KFl relative to mAb 4-4-20/FDS could be directly correlated to interactions surrounding the mouth of the antibody active-site (i.e., the solvent-accessible regions of the CDRs) and the amino acids of the synthetic peptides. In this scenario, attractive electrostatic interactions (e.g., cationic−anionic interactions) were postulated. Increased transition-state enthalpy of the mAb 4-4-20/monofluoresceinated peptide complexes relative to the mAb 4-4-20/FDS complex (which is devoid of carrier residues) was thus due to a greater number of bonds outside the antibody active that had to be broken as the complexes decayed from products to reactants. Enhanced $\Delta S^{\ddagger}$ values of mAb 4-4-20/D12KFl and mAb 4-4-20/R6D6KFl were attributed to greater rotational, translational, and vibrational degrees of freedom of the peptide as the complex decayed relative to the more restricted degrees of freedom of FDS. It was previously demonstrated (Mummert & Voss, 1996) that the secondary forces dictated by these synthetic peptides dramatically affect the fluorescence quenching and absorption properties of the fluorescein/active-site interaction (Table 4). These differences have been interpreted as changes in active-site molecular orientations relative to the fluorescyl moiety and/or changes in the hydration level of the antibody active site. Therefore, we incorporated into this model the concept that binding events at the CDR/peptide interface resulted in perturbations that were translated into the binding pocket of mAb 4-4-20 through bonding networks perhaps indicative of compensatory changes in β-pleated sheet structures.

The first model implied a large degree of orientational freedom of the mAb 4−4-20 CDRs and/or of the amino acids constituting the peptides for productive electrostatic interactions. However, we had no evidence indicating that such orientational flexibility existed. Therefore, a second model was developed in which electrostatic interactions were repulsive. In this scenario, repulsion between the CDRs surrounding the mouth of the antibody active site and the amino acids of the peptides perturbed the primary interaction. Increased $\Delta H^{\ddagger}$ and $\Delta S^{\ddagger}$ values were therefore due to the increased number of bonds within the active site which was a direct result of secondary force-directed perturbations. For example, differences in the levels of hydration within the active site could significantly change the hydrogen bonding potential. Hydration has been shown to significantly impact the free energy of binding (Herron *et al.*, 1995). As noted above, secondary forces altered the environment of the active site as evidenced by spectral measurements (Table 4). Therefore, the second model was considered to have significant merit.

The final model developed considered that an intermediate situation between models 1 and 2 existed. In this case, partial bonding and nonbonding interactions between amino acids of the peptides and accessible regions of the CDRs occurred in addition to changes in the bonding potential of the active site.

Values for $\Delta G^{\ddagger}$ indicated the net energetic barrier that must be crossed for decay of the complex. The height of this barrier denoted the rate at which decay proceeded. The larger the barrier height, the slower the reaction while the smaller the barrier height the faster the reaction. Tables 2 and 3 indicated that $\Delta G^{\ddagger}$ was largest for the decay of the mAb 4-4-20/FDS complex and was smallest for the mAb 4-4-20/R6D6KFl complex. The barrier height ($\Delta G^{\ddagger}$) for the decay of the mAb 4-4-20/R6D6KFl complex was the smallest (+18.77 kcal/mol) and was decreased 2.05 kcal/mol relative to the mAb 4-4-20/FDS complex decay while the mAb 4-4-20/D12KFl barrier (+19.15 kcal/mol) showed a more modest decrease relative to the mAb 4-4-20/FDS complex (1.67 kcal/mol). This result suggested that the unimolecular rate constant should be smallest for mAb 4-4-20 plus fluorescein and greatest for mAb 4-4-20 plus R6D6KFl. This expectation was verified based on the experimentally determined unimolecular rate constants (Table 1) and explains the reported affinity constants for mAb 4-4-20 with these monofluoresceinated peptides (Mummert & Voss, 1996). It had been previously determined that the K_a for mAb 4-4-20 was significantly decreased for D12KFl ($K_a = 1.49 \times 10^9$ M^{-1}) and R6D6KFl ($K_a = 7.47 \times 10^8$ M^{-1}) relative to FDS ($K_a = 3.14 \times 10^{10}$ M^{-1}). Decreased energetic barriers for the monofluoresceinated peptides resulted in increased unimolecular rate constants relative to FDS. Since the bimolecular rate constants for FDS and the monofluoresceinated peptides are invariant (Mummert & Voss, 1996), the net effect of increasing the unimolecular rate constant is to decrease the affinity constant since $K_a = k_1/k_2$ where k_1 is the bimolecular rate constant and k_2 is the unimolecular rate constant. It is of interest to note that even though D12KFl and R6D6KFl had a larger enthalpic contribution in the transition state than FDS the barrier was decreased for D12KFl and R6D6KFl due to the entropic contribution.

The failure of transition-state theory to estimate the rate of decomposition of the mAb 4-4-20/R12KFl complex was the result of theory limitations. Fundamental assumptions of transition state theory are that reactive trajectories cross the transition-state only once and that the reaction occurs on a single energy surface (Winger, 1938; Wolynes, 1987).

Deviations from transition-state theory occur when these criteria are not met and the transmission coefficient (κ) is not equivalent to unity. The value of κ correlates with solvent coupling (inertial regime) and intramolecular dynamics independent of solvent (diffusive regime) (Chandler, 1978; Northrup & Hynes, 1978; Hasha *et al.*, 1982; Doster, 1983). The frictional coefficient in both of these regimes dictates the value of κ (Chandler, 1978; Northrup & Hynes, 1978). Both inertial and diffusive regimes modulate κ in proteins (Doster, 1983). For example, it has been determined that the diffusive regime restricts aromatic ring rotations in the protein interior (McCammon & Karplus, 1979; Karplus & McCammon, 1981). The frictional coefficient imposed on ring orientations due to the surrounding atomic matrix has been used to explain this observation (McCammon & Karplus, 1979; Karplus & McCammon, 1981). It is hypothesized that the failure of transition-state theory to approximate the decay of the mAb 4-4-20/R12KFl complex was the result of the inertial and/or diffusive regimes. We concieved that the secondary forces dictated by R12KFl resulted in greater perturbation of the antibody variable domains than the secondary forces dictated by either D12KFl or R6D6KFl. A simplistic rationale for the differences in secondary (forces) directed perturbations was developed based on the the volume differences of D and R. The van der Waals volume for R $\sim$ 148 Å^3 while the van der Waals volume for D $\sim$ 91 Å^3 (Richards, 1974). The greater volume of the R12KFl peptide results in a greater displacement of the variable domain atomic coordinates than either D12KFl and R6D6KFl. Displacement of the atomic coordinates results in a value of κ that differs from unity due to the frictional coefficient in inertial and/or diffusive regimes. It is important to note that this argument does not suggest that D12KFl and R6D6KFl do not cause secondary force-directed atomic coordinate displacement. Perurbations caused by R6D6KFl and D12KFl were, however, adequately approximated by transition-state theory.

In conclusion, this study suggested that secondary forces of the mAb 4-4-20/monofluoresceinated peptide modulated binding interactions via increased transition-state enthalpic and entropic contributions. The net result was a decreased energetic barrier that allowed modulation of the previously reported affinity constants of mAb 4-4-20 for the monofluoresceinated peptides due to variation of the unimolecular rate constant. Spectral measurements have indicated that secondary forces dictate the metatypic state (Mummert & Voss, 1995, Mummert 1996). This contention was supported by the scenario presented by the mAb 4-4-20/R12KFl complex decay. We assumed the failure of transition-state theory to approximate the activation enthalpy and entropy was due to a value of κ that differed from unity. This difference in turn was assumed to be a result of the frictional coefficient in the inertial and/or the diffusive regimes which corresponded to displacement of the variable domain atomic coordinates. The finding that D12KFl and R6D6KFl complex decays could be approximated by transition-state theory, but R12KFl could not, suggested that secondary forces in the system investigated differentially perturbed the variable domains of mAb 4-4-20.

When considering the above arguments, the following concepts must be considered: (1) the various substates of the variable domains and the ligands were thermally averaged; (2) the barriers crossed during complex decays were thermally averaged; and (3) the values for $\Delta G^{\ddagger}$, $\Delta H^{\ddagger}$, and $\Delta S^{\ddagger}$ are the upper limits of the system since solvent was considered as a part of the system (Beece *et al.*, 1980).

REFERENCES

Absolom, D. R., & van Oss, C. J. (1986) *Crit. Rev. Immunol. 6*, 1−46.

Ansari, A., Jones, C. M., Henry, E. R., Hofrichter, J., & Eaton, W. A. (1992) *Science 256*, 1796−1798.

Beece, D., Eisenstein, L., Frauenfelder, H., Good, D., Marden, M. C., Reinisch, L., Reynolds, A. H., Sorensen, L. B., & Yue, K. T. (1980) *Biochemistry 19*, 5147−5157.

Carrero, J., & Voss, E. W., Jr. (1996) *J. Biol Chem.* (in press).

Chandler, D. (1978) *J. Chem. Phys. 68*, 2959−2970.

Coelho-Sampaio, T., & Voss, E. W. Jr. (1993) *Biochemistry 32*, 10929−10935

Doster, W. (1983) *Biophys. Chem. 17*, 97−103.

Eyring, H. (1935) *J. Chem. Phys. 3*, 107−115.

Frauenfelder, H. (1979) in *Tunneling in Biological Systems* (Chance, B., DeVault, D. C., Frauenfelder, H., Marcus, R. A., Schriefer, J. R., & Sutin, N., Eds.) pp 627−649, Academic Press, Inc., New York.

Frauenfelder, H., Parak, F., & Young, R. D. (1988) *Annu. Rev. Biophys. Biophys. Chem.*, 451−479.

Frauenfelder, H., Nienhaus, G. U., & Johnson, J. B. (1991) *Ber. Bunsen-Ges. Phys. Chem. 95*, 272−278.

Gulliver, G. A., Rumbley, C. A., Carrero, J., & Voss, E. W., Jr. (1995) *Biochemistry 34*, 5159−5163.

Hasha, D. L., Eguchi, T., & Jonas, J. (1982) *J. Am. Chem. Soc. 104*, 2290−2297.

Hazen, S. J., Hofüchter, J., & Eaton, W. A. (1995) *Science 269*, 959−962.

Herron, J. N. (1984) in *Fluorescein Hapten: An Immunological Probe* (Voss, E. W., Jr., Ed.) pp 50−75, CRC Press, Inc., Boca Raton, FL.

Herron, J. N., Kranz, D. M., Jameson D. M., & Voss, E. W., Jr. (1986) *Biochemistry 25*, 4602−4609.

Herron, J. N., He, X.-M., Mason, M. L., Voss, E. W., Jr., Edmundson, A. B. (1989) *Proteins: Struct., Funct., Genet. 5*, 271−280.

Herron, J. N., Johnston, T. S., He, X.-M., Guddat, L., Voss, E. W., Jr., & Edmundson, A. B. (1994) *Biophys. J. 67*, 2167−2183.

Karplus, M. A., & McCammon, J. A. (1981) *FEBS Lett. 131*, 34−36.

Kranz, D. M., & Voss, E. W., Jr. (1981) *J. Biol. Chem. 257*, 6987−6995.

McCammon, J. A., & Karplus, M. (1979) *Proc. Natl. Acad. Sci. U.S.A. 76*, 3585−3589.

Miklasz, S. D., Gulliver, G. A., & Voss, E. W., Jr. (1995) *J. Mol. Recognit. 8*, 258−269.

Moore, J. W., & Pearson, R. G. (1981) in *Kinetics and Mechanism*, 3rd ed., pp 137−188, John Wiley & Sons, Inc., New York.

Mummert, M. E., & Voss, E. W., Jr. (1995) *Mol. Immunol. 32*, 1225−1233.

Mummert, M. E., & Voss, E. W., Jr. (1996) *Mol. Immunol.* (submitted for publication).

Northrup, S., & Hynes, J. T. (1978) *J. Chem. Phys. 69*, 5246−5260.

Richards, F. M. (1974) *J. Mol. Biol. 82*, 1−14.

Tetin, S. Y., Mantulin, W. W., Denzin, L. K., Weidner, K. M., & Voss, E. W., Jr. (1992) *Biochemistry 31*, 12029−12034.

Voss, E. W., Jr. (1993) *J. Mol. Recognit. 6*, 51−58.

Voss, E. W., Jr., Dombrink-Kurtzman, M. A., & Miklasz, S. D. (1988) *Immunol. Invest. 17*, 25−39.

Weidner, K. M., Denzin, L. K., Kim, M. L., Mallender, W. D., Miklasz, S. D., & Voss, E. W., Jr. (1993) *Mol. Immunol. 30*, 1003−1011.

Whitlow, M., Howard, A. J., Wood, J. F., Voss, E. W., Jr., & Hardman, K. D. (1995) *Protein Eng. 8*, 749−761.

Winger, E. (1938) *Trans. Faraday Soc. 34*, 29−41.

Wolynes, P. (1987) in *Protein Structure: Molecular and Electronic Reactivity* (Austin, R., Buhks, E., Chance, B., DeVault, D., Dutton, P. L., Frauenfelder, H., & Gol'danskii, V. I., Eds.) pp 201−209, Springer-Verlag, Inc., New York.

Wynne-Jones, W. F. K., & Eyring, H. (1935) *J. Chem. Phys. 3*, 492−502.

BI9604791